Journal of Thermal Analysis and Calorimetry, Vol. 57 (1999) 391-400

CALORIMETRIC CONTROL OF ALUMINIUM CASTING QUALITY*

C. M. Allen[1], *K. A. Q. O'Reilly*[1], *B. Cantor*[1] *and P. V. Evans*[2]

[1]Oxford Centre for Advanced Materials and Composites, Department of Materials University of Oxford, Parks Rd, Oxford OX1 3PH
[2]Alcan International Ltd., Banbury Laboratory, Southam Rd., Banbury, Oxon. OX16 7SP, UK

Abstract

Differential scanning calorimetry (DSC) combined with an entrained droplet technique [1] has been successfully used on a series of melt spun alloys with deliberate impurity additions to study the nucleation related aspects of secondary phase selection during solidification of dilute Al alloys. This paper illustrates how DSC is a sensitive tool for determining the effect impurities can have on the nucleation of secondary phases, and hence material properties of these alloys. Stepped cooling/isothermal holding profile DSC has also been used in preliminary investigations of the thermodynamic range of formation of the Al–Fe eutectic phases and their nucleation and growth solidification kinetics.

Keywords: Al alloys, casting, entrained droplet technique, nucleation, secondary phase selection

Introduction

Approximately ten million tonnes of ingot for rolled Al products is cast annually. For commercial purity (1xxx series) alloys used in applications including packaging, anodised sheet for architectural use and lithographic printing sheet, alloying additions (typically Fe and Si) and impurities together commonly constitute <1 wt% of the alloys. The as-solidified microstructure typically contains ~1 vol% of Al-Fe-Si eutectic secondary phase particles. These particles are important as they can influence material properties, such as strength, resistance to fracture, ductility and surface electrochemistry, which in turn affect downstream processing requirements and final product quality. Variations in solidification conditions during the casting process [2–4] lead to variations in secondary phase content, size and morphology, by changing the nucleation and growth mechanisms that operate [5]. The outermost part of the cast is commonly scalped off to remove the uneven cast surface and inverse segregation zone. In surface critical applications the remaining material has to be homogenised to minimise the variations in secondary phase content, which would otherwise affect the surface quality at final gauge.

* Award lecture, presented at ESTAC-7, Balatonfüred, Hungary

1418–2874/99/ $ 5.00

Akadémiai Kiadó, Budapest
Kluwer Academic Publishers, Dordrecht

The secondary phase particles form via eutectic reactions in the final ~5–15 vol% of liquid, which by that stage is present in the form of an interdendritic network or possibly as isolated puddles between the solid aluminium dendrite arms. Eutectic solidification does not proceed spontaneously once below the eutectic temperature, but requires a catalyst to nucleate solidification. Liquid divided up into puddles requires a large number of catalysts for solidification to proceed to completion. Consequently the range of nucleants available, and hence ppm levels of certain trace impurities, can have a significant influence on the nucleation of secondary phases during solidification and the resulting material properties.

The low volume fraction, often submicron size, similar growth morphologies and wide range of possible secondary phases renders their identification by conventional techniques such as transmission electron microscopy (TEM) or X-ray diffraction (XRD) laborious, time consuming and potentially inaccurate. This paper reviews how differential scanning calorimetry (DSC) can be used to provide a simpler, faster and more sensitive means of studying both secondary phase identity and the mechanisms of their formation.

Experimental

A modified entrained droplet method [1] combined with differential scanning calorimetry (DSC) has been previously used by Cantor and co-workers [6] to study the heterogeneous nucleation of solidification of one phase by another under clean conditions, by segregating impurities into an insignificant fraction of the total liquid. In this work the dispersion is manipulated to accentuate the effects of the deliberately added impurities, exaggerating the nucleation aspects of the solidification of that liquid lying between the Al dendrite arms during the final stages of solidification in commercial casting operations.

Commercial purity alloys and high purity model Al–Fe–Si alloys with deliberate impurity additions were manufactured by melting the components in a resistance furnace and then casting into steel moulds. Approximate 5 g samples were remelted in quartz crucibles under $4.5 \cdot 10^4$ Pa Ar and melt-spun when at >800°C by ejection through a 1 mm nozzle using an overpressure of $1.5 \cdot 10^4$ Pa Ar onto a Cu wheel rotating at 23 m s^{-1}. All resulting ribbons were typically 0.1–1 m long, <5 mm wide and 50–150 μm thick.

Approximate 2 mg specimens of these ribbons were sealed into either Mo or W lined Cu pans and analysed in either a Mettler-Toledo 821e DSC or a TA Instruments 2010 DSC, using an identically prepared Mo or W lined empty Cu pan as a reference. Two cycles of closely controlled eutectic melting and resolidification of the secondary phase particles, were performed under a dynamic Ar atmosphere, by heating from 632–658°C at 2 K min^{-1}, resolidifying at 2 K min^{-1} to 632°C, and then remelting and resolidifying once more in an identical manner. This technique is illustrated schematically in Fig. 1. The low heating and cooling rates of 2 K min^{-1} have to be used to sufficiently resolve the overlapping melting peaks of the eutectic melting of the secondary phases, which occurs within ≤9 K of the melting of the Al matrix. By solidifying in a series of stepped isothermal holds at 0.5 K intervals, of 2.5–

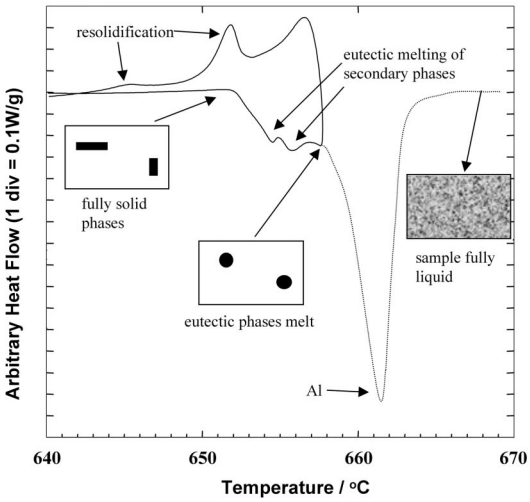

Fig. 1 Schematic of eutectic melting and resolidification DSC trace (solid line) compared to full melting trace (dashed line) of specimen

15 min duration, and comparing the heat flows obtained to those seen on continuous cooling, information about the thermodynamics and kinetics of eutectic solidification could also be obtained.

Eutectic melting forms a dispersion of entrained liquid droplets. Careful temperature control is also necessary, as insufficient heating melts too small a proportion of the eutectic phases and does not form isolated liquid puddles, and excessive heating leads to coarsening and coalescence of the puddles [7]. As the droplets are dispersed throughout the solid Al matrix, each droplet requires its own nucleant for solidification. The subsequent resolidification of the droplets, as studied using DSC, can then be used to investigate the nucleation component of solidification in isolation.

Solidification microstructures were investigated in two ways. Firstly, by quenching DSC specimens at different stages during resolidification after partial melting, then mounting and polishing them for metallographic analysis. Secondly, by extracting as solidified secondary phase particles from the alloys by dissolving the Al matrix in boiling butanol under pressure [8–12], mounting the particles on an amorphus C film and analysing them in the TEM [13].

Results and discussion

As melt-spun microstructures

Figure 2 shows a typical melt spun microstructure, consisting of submicron particles dispersed both within the Al cells and along the Al cell boundaries [14]. As Fig. 2 shows, melt spinning successfully achieves the initially high degree of secondary phase dispersion necessary for subsequent entrained droplet studies.

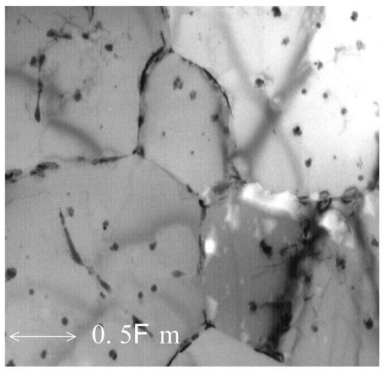

Fig. 2 TEM micrograph of as melt spun ribbon microstructure, showing dispersion of submicron secondary phase particles within Al cells and along cell boundaries

Effect of heat treatment on secondary phase content

Figure 3 shows a typical set of DSC melting endotherms from a series of Al–0.3Fe–0.1Si ribbons with different impurity additions as shown. As Fig. 3 shows, the melting behaviour of all the ribbons is similar. This indicates that any differences that existed in the secondary phase contents of the different composition ribbons in the as spun condition have been removed via microstructural equilibration during heating in the DSC prior to melting [15]. This equilibration consists of transformation of metastable Al–Fe(–Si) phases to the equilibrium Fe_4Al_{13} phase, and precipi-

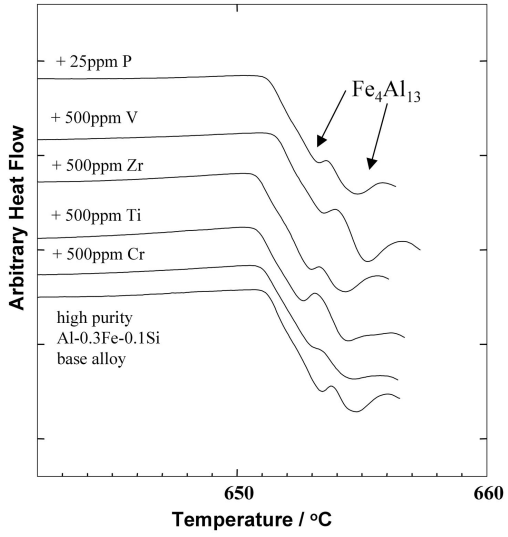

Fig. 3 DSC eutectic melting endotherms from Al–0.3Fe–0.1Si ribbons with no additions and additions of P, V, Zr, Ti and Cr. Both melting peaks correspond to the eutectic melting of the equilibrium Al–Fe_4Al_{13} (or Al–$FeAl_3$) eutectic

tation of excess solute also as Fe_4Al_{13}. TEM indicates (not shown) that these processes result in two distinct morphologies of Fe_4Al_{13}, explaining the double peak observed in the DSC melting endotherms from all the ribbons. Consequently, impurity additions do not affect the secondary phase content of the heat treated ribbons.

Secondary phase content following eutectic melting and resolidification

Figure 4 shows a typical set of DSC solidification exotherms from a series of Al–0.3Fe–0.1Si ribbons with different impurity additions as shown following eutectic melting of the secondary phases. As Fig. 4 shows, the solidification behaviour is different with different impurity additions. In particular, the addition of V mimics the solidification of a commercial purity alloy melt spun, melted and resolidified under identical conditions [13, 16]. Figure 5 shows a set of DSC solidification exotherms from a series of Al–0.3Fe–0.1Si–(0.001–0.05V) ribbons compared to the solidification exotherm from a commercial purity ribbon. As shown in Fig. 5, TEM examination of extracted particles shows that the higher temperature peak common to all exotherms corresponds to the resolidification of the equilibrium Al–Fe_4Al_{13} eutectic [16]. As also shown in Fig. 5, TEM examination of extracted particles shows that the lower temperature peak in the exotherms from the commercial purity ribbon and the high purity ribbon with 500 ppm V addition corresponds to the eutectic solidification of the metastable Al–$FeAl_m$ eutectic [16]. This phase is known to contribute to the fir tree defect in commercial castings [2]. DSC is capable of detecting its formation in as little as ~0.1 vol% of the microstructure (or 10% of the secondary phase population), illustrating the high sensitivity of DSC.

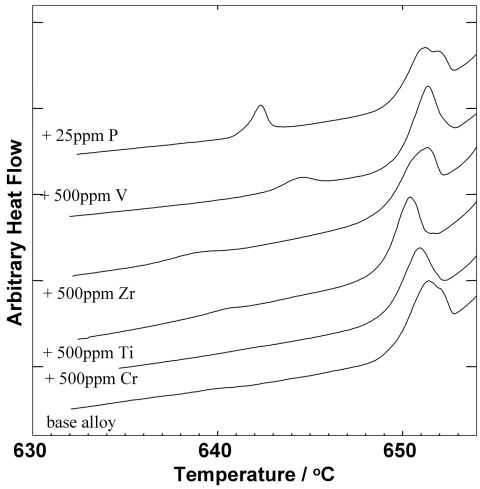

Fig. 4 DSC eutectic resolidification exotherms following eutectic melting from Al–0.3Fe–0.1Si ribbons with no additions and additions of P, V, Zr, Ti and Cr. The higher temperature peak is common to all exotherms, although the shape is different for different ribbon compositions. The lower temperature peak changes both shape and position with different ribbon composition

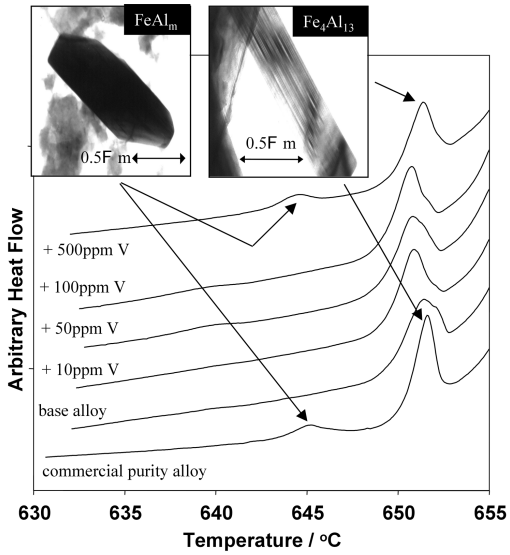

Fig. 5 DSC eutectic resolidification exotherms following eutectic melting from Al–0.3Fe–0.1Si ribbons with no additions, and with V additions of 10, 50, 100 and 500 ppm, compared to the exotherm from a commercial purity Al–0.3Fe–0.1Si ribbon. TEM examination shows that the higher temperature peak common to all exotherms corresponds to the eutectic resolidification of the equilibrium Al–Fe_4Al_{13} (or Al–$FeAl_3$) eutectic. The lower temperature peak present in the exotherms from the Al–0.3Fe–0.1Si–0.05V ribbon and commercial purity ribbon corresponds to the eutectic resolidification of the metastable Al–$FeAl_m$ eutectic

Microstructural location of solidification events

Figure 6 shows the same set of DSC solidification exotherms as shown in Fig. 5, with corresponding backscattered electron micrographs of intracellular and cell boundary secondary phase particle morphologies when quenched from the points indicated during solidification [13]. The fine scale eutectic structure present in both the intracellular and cell boundary phases when quenched from above the Al–Fe_4Al_{13} resolidification peak indicate that the eutectic in both locations was liquid at the point of quench. The absence of the fine scale eutectic structure in the cell boundary phases when quenched from below the Al–Fe_4Al_{13} resolidification peak indicates that the Al–Fe_4Al_{13} eutectic solidified predominantly on the cell boundaries. The presence of the fine scale eutectic structure in the intracellular phases when quenched from below the Al–Fe_4Al_{13} resolidification peak indicates that these were still liquid at the point of quench. The replacement of the fine scale eutectic structure by a blockier morphology in the intracellular phases when quenched from below the Al–$FeAl_m$ resolidification peak indicates that the Al–$FeAl_m$ eutectic solidified predominantly within the intracellular liquid puddles.

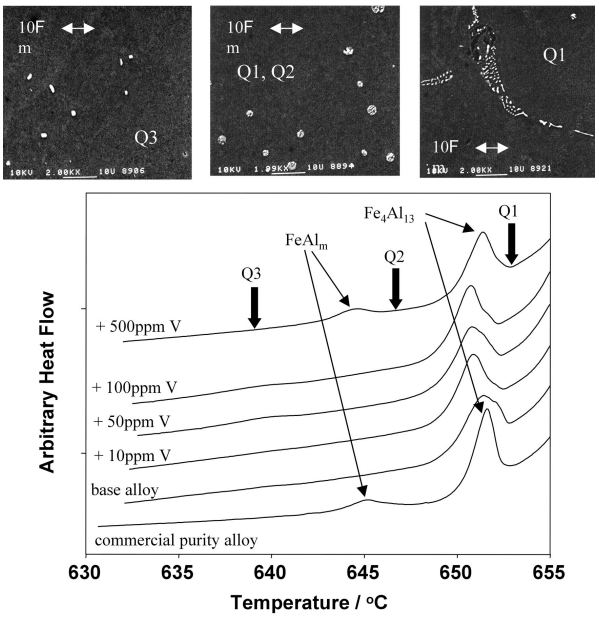

Fig. 6 DSC eutectic resolidification exotherms following eutectic melting from Al–0.3Fe–0.1Si ribbons with no additions, and with V additions of 10, 50, 100 and 500 ppm, compared to the exotherm from a commercial purity Al–0.3Fe–0.1Si ribbon. Both the cell boundary and intracellular phases have a fine scale eutectic structure when the sample is quenched from Q1. Only the intracellular phases have this structure when quenched from Q2. The intracellular phases have a blockier structure when quenched from Q3

Preliminary study of Al–Fe_4Al_{13} solidification kinetics

Figure 7 shows a time-temperature profile (dashed line) and resulting heat flows (solid line) for a 5 min/0.5 K stepped cooling profile following eutectic melting. When the sample is fully solid, a sudden 0.5 K change of temperature produces a rapid (short time) exotherm of constant size, relating to the specific heat capacity of the sample. When the eutectic is fully molten and only the primary Al matrix solidifies in each step, a superposition of a rapid heat capacity related heat flow and a rapid heat flow relating to a progressively smaller and smaller liquid fraction of primary Al is detected as the temperature is stepped down. This indicates that the nucleation and subsequent growth of the liquid Al on the existing solid Al has little if any kinetic barrier, as would be anticipated given that the nucleant and nucleated, growing phase are the same. During the Al–Fe_4Al_{13} eutectic solidification however, there are kinetic (time dependent) lags seen in the heat flow, indicating that the nucleation and/or growth of the eutectic is not instantaneous, despite the facts that one of the eutectic phases is Al (and so should be readily nucleated) and that the cooling rate is very low so the undercooling required for growth of the eutectic phase should be negligible [17]. This may explain why the Al–Fe_4Al_{13} eutectic is displaced by the Al–$FeAl_m$ in the intracellular puddles in certain ribbons.

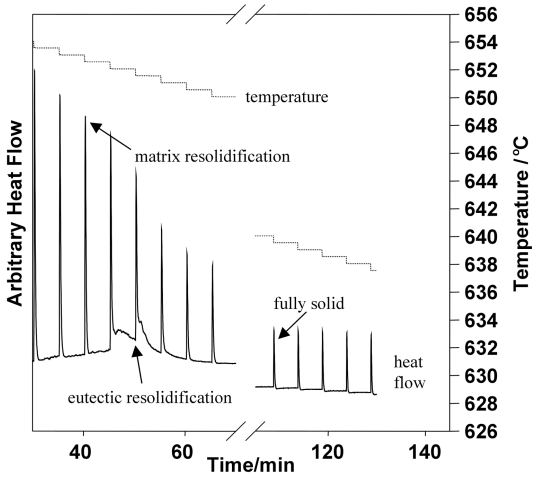

Fig. 7 Temperature-time (dashed line) and corresponding heat flow-time (solid line) curves for Al–Fe_4Al_{13} eutectic solidification during a stepwise isothermal cooling program. Eutectic resolidification is both temperature and time dependent. Matrix resolidification is virtually time independent

Figure 8 shows plots of total heat flow measured vs. temperature interval for 0.5 K steps of duration in the range 2.5–15 min. As the isothermal hold time per step increases there is more time per step for solidification to proceed to completion, and consequently the temperature range over which Al–Fe_4Al_{13} eutectic solidification is observed reduces to a minimum of two steps or ~1 K. This represents the thermody-

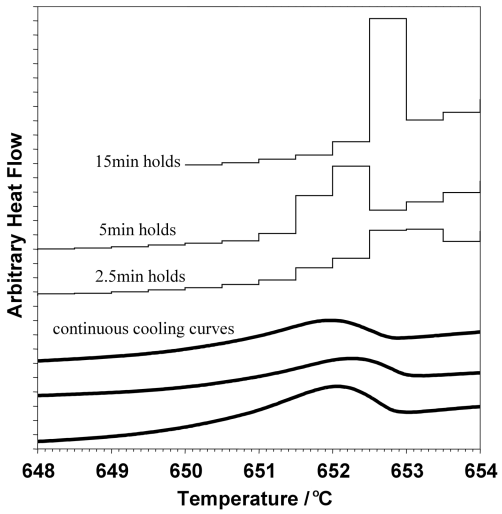

Fig. 8 Heat flow-temperature curves for heat released from Al–Fe_4Al_{13} eutectic solidification during stepwise cooling *vs.* continuous cooling. Profile of stepwise cooling curves tend to that of continuous cooling curves as step duration decreases

namic temperature range of solidification of the eutectic. Solidification then takes ~30 min to proceed to completion. As the time per step decreases to 2.5 min, there is insufficient time for solidification to proceed to completion in each step, and the temperature range increases to ~5 steps or ~2.5 K. This range matches more closely that observed on continuous cooling at 2 K min^{-1}, indicating that thermodynamic equilibrium is not maintained during continuous solidification at 2 K min^{-1}. The total time for solidification then reduces to ~12.5 min.

Conclusions

The entrained droplet technique provides a successful experimental means of studying the nucleation related aspects of phase selection during the final stages of solidification in dilute alloys. DSC analysis of solidification supports existing TEM based phase identification techniques, and is an easier, more rapid and sensitive means of identifying secondary phase contents down to <0.1 vol%. Application of these techniques to melt spun alloys with deliberate impurity additions indicates that impurities influence the nucleation behaviour of resolidification after eutectic melting, thereby providing a means of influencing secondary phase content. In particular, V assists the formation of the metastable $FeAl_m$ phase in the ribbons, which is the phase known to be associated with the occurrence of macroscopic fir tree zones in commercial castings.

Stepped cooling/isothermal holding DSC has been demonstrated to be a means to investigate the thermodynamic range of formation of the Al–Fe eutectic phases and their nucleation and growth solidification kinetics. A better understanding of these parameters will allow secondary phase content to be further manipulated in the future.

* * *

We would like to thank the UK Engineering and Physical Sciences Research Council and Alcan International Ltd. for financial support, and J. Worth, A. Flemming and J. Brown of Alcan International Limited for their guidance and assistance in the preparation of alloys, in secondary phase extraction and EDX analysis, and in WDX/EPMA analysis respectively.

References

1 C. C. Wang and C. S. Smith, Trans. Met. Soc. AIME, 188 (1950) 136.
2 H. Westengen, Z. Met., 73 (1982) H.6, 360.
3 P. Skjerpe, Met. Trans., 18A (1987) 189.
4 H. Kosuge, Keikinzoku, 34 (1984) No. 4.
5 S. Brusethaug, D. Porter and O. Vorren, Hydro Aluminium, Suundal Verk, paper presented on ILMT, 1987, 477.
6 B. Cantor, J. Thermal Anal., 42 (1994) 647.
7 C. M. Allen, K. A. Q. O'Reilly and B. Cantor, in preparation.
8 M. Ryvola and L. R. Morris, from 'Microstructural Science, Vol. 5', edited by J. Braun, H. W. Arrowsmith and J. L. McCall, Elsevier, North Holland, 1977.
9 J. Howe, Metallography, 16 (1983) 275.
10 C. J. Simensen, P. Fartum and A. Andersen, Z. Anal. Chem., 319 (1984) 286.
11 J. Strid and C. J. Simensen, Pract. Met., 23 (1986) 485.

12 A. Oscarsson, W. B. Hutchinson, H.-E. Ekström, D. P. E. Dickson, C. J. Simensen and G. M. Raynaud, Z. Met., 79 (1988) H.9, 600.
13 C. M. Allen, K. A. Q. O'Reilly, B. Cantor and P. V. Evans, submitted to Acta Met.
14 C. M. Allen, K. A. Q. O'Reilly, B. Cantor and P. V. Evans, Mat. Sci. Forum, 217-222 (1996) Part 2, 679.
15 C. M. Allen, D. Phil. Thesis, Oxford University, UK, 1997.
16 C. M. Allen, K. A. Q. O'Reilly, B. Cantor and P. V. Evans, Mat. Res. Soc. Symp. Proc., 481 (1998) 3.
17 D. Liang and H. Jones, Z. Met., 83 (1992) 224.